Energy and Environment Research; Vol. 12, No. 1; 2022
ISSN 1927-0569 E-ISSN 1927-0577
Published by Canadian Center of Science and Education

A Novel Integrated Design for Heat and Water Recovery from Exhaust Flue Gas of Bandar Abbas Power Plant

Erfan Ghamati[1] & Javad Mirrezaie Roudaki[1]

[1] Department of Energy and Mechanical Engineering, Shahid Beheshti University, Tehran, Iran

Correspondence: Erfan Ghamati, Department of Energy and Mechanical Engineering, Shahid Beheshti University, Abbaspour complex, Tehran, Iran.

Received: April 24, 2022 Accepted: May 19, 2022 Online Published: May 30, 2022

doi:10.5539/eer.v12n1p26 URL: https://doi.org/10.5539/eer.v12n1p26

Abstract

This study concerns a theoretical design of a condensing heat exchanger for a 320 MW unit of Bandar Abbas thermal power plant in the south of Iran. A film theory in conjunction with heat and mass transfer analogy is used as the theoretical basis of the design. The condensing unit is used for heat and mass recovery from the natural gas-fired boiler flue gases. The assumed condensing unit includes 4 equal capacity condensing heat exchangers, each of which is supposed to reduce the flue gas temperature from 160 ℃ to 53℃. Decreasing the flue gas temperature to below the dew point temperature of its water vapor causes condensation (latent) and sensible heat transfer. The analysis was done for 13%, 15%, and 17% of the water vapor volume fraction in the flue gases, and based on the 17% water vapor fraction, 52.8 tons/hr of water was recovered. This recovered water could be used as the cooling tower makeup, and accordingly, almost 14% of water consumption is saved. The recovered heat by the condensing unit is also being used as the heat source of an ORC cycle, and up to 2.8 MW power is estimated to be generated depending on the evaporation temperature.

Keywords: Condensing heat exchanger, latent heat recovery, Organic Rankine Cycle (ORC), waste heat recovery, water recovery

1. Introduction

Energy and water shortage are of the immense life challenges worldwide. The issues of waste heat and water recovery have attracted attention as part of efficiency improvement in energy plants by different CHP methods (Wang, Husnain & Fareed, 2019; Chen, Finney, Zhang, Zhou, Sharifi & Swithenbank, 2012). Steam power plants are larger consumers of water than any other industry (Xiong, Niu, Tan, Liu & Wang, 2014). The electricity demand is ever-growing, which consequently enhances water demands for power generation. As result, water availability issues are becoming increasingly important. The exhaust flue gas of a power plant boiler is wasted in the atmosphere with a temperature normally above 150℃. For a 600 MW power plant, the flue gas flow rate is about 2.87 million kg/hr, and 10-20 % of the flue gas volume is water vapor. This considerable waste stream can be a great source of water and energy (Goel, 2012; Comakli, 2008; Terhan & Comakli, 2016).

The exhaust flue gases from boilers contain a significant amount of energy and water vapor that is wasted in the environment. The discharged heat with the flue gases accounts for about 50-80 percent of boiler heat losses, and a large percent of the heat loss is due to the latent water vapor. Therefore, the boiler efficiency could be potentially improved by recovering the waste heat and water vapor. To recover the latent heat of water vapor, the temperature of the flue gases must be reduced to a level lower than the dew point of the water vapor. The water vapor concentration is based on the fuel type which is fired in the boiler. Water vapor concentration is 11-13, 13-17 and 10-20 percent by volume for oil-fired, natural gas-fired, and coal-fired boilers, respectively. An increase in the flue gas water vapor volume fraction causes the dew temperature to rise (Goel, 2012; Levy, Bilirgen, Jeong, Kessen, Samuelson & Whitcombe, 2008). In general, the flue gas water vapor dew point temperature is about 50-60 ℃ (Levy, Bilirgen, Jeong, Kessen, Samuelson & Whitcombe, 2008). The exact amount of this temperature depends on the percentage of excess air used in the combustion process. Therefore, condensing the flue gas's water vapor can recover its sensible and latent heat, and the condensed water could be used again (Goel, 2012). Exhaust flue gases with a water vapor volume fraction more than 10 % and a temperature above 120 ℃ attracted growing interest in waste heat and water extraction (Zhao, Yan, Wang, Wei, Qi & Wu, 2017; Wang, He, Sun, Wu, Yan & Pei, 2012).

The best way to recover the exhaust flue gas's heat and water is to use condensing heat exchangers (Huang, Zheng, Baleynaud & Lu, 2017; Levy, Bilirgen, Kessen, Hazell & Carney, 2011). The condensing heat exchanger uses a cooling fluid to decrease the flue gas temperature to a level below the water vapor dew point. Thus, water vapor can be condensed, and both sensible and latent heat is transferred to the cooling fluid. Therefore, waste heat and water can be recovered. In the case of power plants, the heat that is recovered by condensing heat exchanger can be used for combustion air and boiler feed water preheating and utilities or as a heat source for an ORC cycle. These applications of recovered heat lead to a decrease in the power plant heat rate and fuel consumption and an increase in the boiler efficiency (Levy, Bilirgen, Jeong, Kessen, Samuelson & Whitcombe, 2008). Condensing heat exchangers can recover 50 percent of waste energy in flue gases (Cortina, 2006).

Chen, Finney, Zhang, Zhou, Sharifi and Swithenbank (2012) technically and economically investigated the feasibility of recovering heat and water vapor from exhausted flue gases of a 40 MW boiler. By using an indirect heat exchanger, the flue gas temperature was decreased to 30℃. In order to avoid corrosion, heat exchange tubes were coated with polypropylene carbon steel. The coating caused an increase in thermal resistance and then an increase in the heat exchanger area. According to present reliable value results, the cash return period of a stainless heat exchanger is longer than that of a carbon steel heat exchanger.

Cho, Lee, Kang, Jung, Lee, Kharangate, Ha, Huh and Lee (2022) studied the condensation in the presence of non-condensable gases on a circular tube. They developed a data base included geometric parameters and operational conditions: air mass fraction, tube diameter, tube length, total pressure, wall sub cooling temperature, average condensation heat transfer coefficient and Reynolds number of the film. The data base was used in a multilayer perception neural network model for predicting the heat transfer coefficient in the condensation.

Gundermann, Raab and Botsch (2021) experimentally investigated a correction factor that could calculate the heat transfer coefficient in the condensation at the presence of non-condensable gases. The presented correction factor depends on the water vapor volume fraction, the Reynolds number and the geometry ration between the inner diameter and the tube length.

Mohammadaliha, Amini and Bahrami (2020) analyzed the pipe thermal conductivity effect on the performance of a condensing heat exchanger in the presence of corrosive substances. They found that thermal conductivity bigger than o.75 $W.m^{-1}.k^{-1}$ has no effect on performance improvement. Therefore materials such as natural graphite, plastics, polymers and ceramics can be used in condensing heat exchangers manufacturing.

Jeong, Kessen, Bilirgen, and Levy (2010) evaluated the flue gas and heat and water recovery experimentally and theoretically. They described a heat and mass transfer process for designing a condensing heat exchanger. The results of the pilot scale and theoretical model were almost the same.

Nabati (2011) studied the water vapor condensation in flue gas with high CO_2 concentration. He explored a simple vertical plane to easily solve and focus on the physical model. He developed two condensation models and used a numerical approach to implement these models. His results showed that the combination of developed condensation models with the numerical solution can model the water vapor condensation behavior together with non-condensable gases. The results of this study can be used to design power plant condensing heat exchangers.

Wang, Husnain and Fareed (2019) investigated the condensation of a turbulent flue gas water vapor numerically and experimentally. They used a mixture of water vapor produced by a steam generator and hot air as flue gas for the experimental setup. The numerical model was studied in ANSYS-FLUENT. There was a good harmony between numerical and experimental results. Their results showed that the major thermal resistance in the condensing heat exchanger originates from the gas side.

Li, Yan, Zhang , Chen, Cui, Song, Chang and Ma (2016) studied the performance of a 300MW coal-fired power plant thermally and economically. They used a direct contact condensation heat exchanger to recover the sensible heat, latent heat, and water vapor from the boiler exhaust flue gases. In this type of condensation, the flue gas desulfurization scrubber is used as a cooling exchanger and minimizes the problems caused by acid condensation in the flue gas. Based on currently available values, this type of flue gas condensation can be profitable in the case of coals with high-moisture concentration.

Terhan and Comakli (2016) designed a heat and water recovery heat exchanger for the flue gas of a 60 MW boiler and conducted an economic analysis. By using the designed heat exchanger, the temperature of flue gas reduced from 160 ℃ to 40℃. The recovered heat was transferred to the cooling water and caused a temperature increase from 10 ℃ to 60℃. The heated water could obtain 184 flats' needs for hot water. The efficiency of

water vapor condensation was reported as 17.8%, and the payback of reducing fuel consumption was calculated at about 40700 $/year.

Kessen (2012) designed an optimal air-cooled condensation heat exchanger for heat and water vapor recovery from exhausted flue gas of a power plant boiler. Both bare and fin tubes were used in the heat exchanger. The efficiency of water vapor condensation was reported as 50 percent.

Maalouf, Ksayer and Clodic (2016) investigated electricity generation with an Organic Rankine Cycle using the recovered heat of industrial low-temperature flue gases. They used an indirect condensation heat exchanger and studied the cycle performance in different flue gas water vapor dew point and evaporator temperatures.

2. Theoretical Analysis

2.1 Condensing Heat Exchanger

In a condensing heat exchanger (CHE), when the tube wall temperature goes below the dew point temperature of water vapor in flue gas, the condensation proceeds as a result of combined heat and mass transfer. Typically, the heat exchanger is divided into two zones, including the non-condensing and condensing zones. These zones should be studied separately. The reason is that only heat transfer occurs in the non-condensing zone. However, both heat and mass transfer are observed in the condensing zone due to vapor condensation.

As shown in Figure1, when the condensation starts, a film of condensate covers the tube surface, and an interface forms between liquid and flue gas. Water vapor in the gas bulk diffuses toward the liquid-gas interface. The non-condensable gases' mass fraction increases along the tube wall as the water vapor mass fraction decreases.

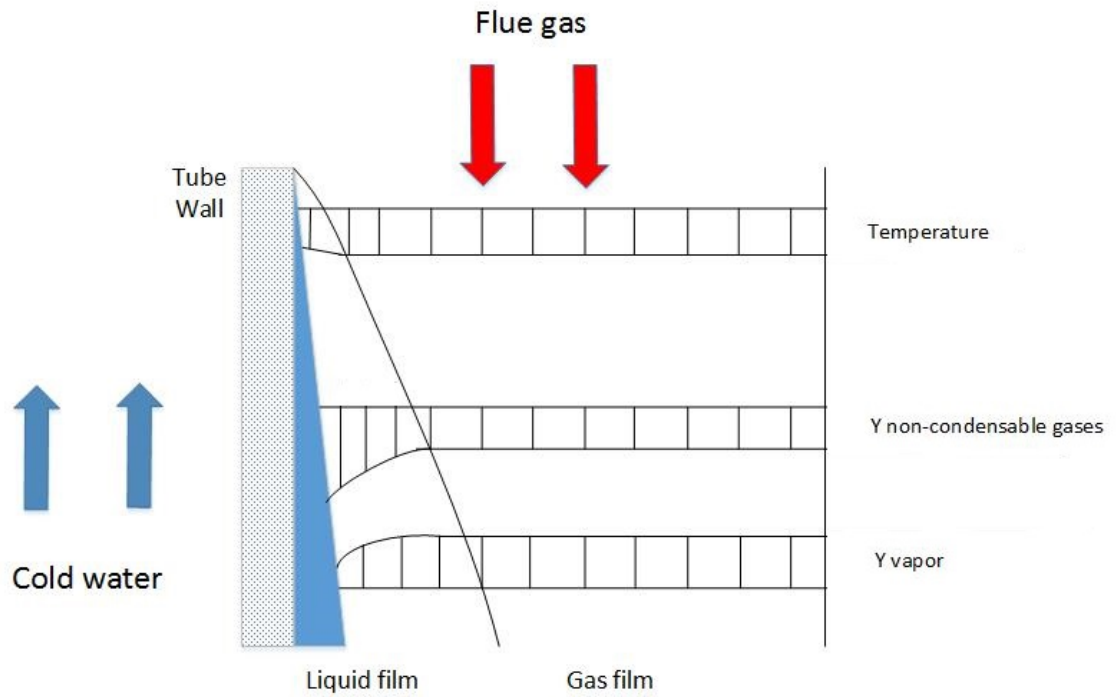

Figure 1. Water vapor condensation in the flue gas

In order to model the condensation of mixtures, a common assumption is the equilibrium of vapor and liquid at the interface. The use of film theory has proven to be more accurate for designing vapor condensers in the presence of non-condensable gases compared to the solution of the conservation equations. This method was first introduced by Colburn and Hougen and then completed by Colburn and Drew.

The transferred heat flux from the gas bulk to the cooling water includes three heat transfer types, namely the sensible heat due to water vapor cooling, the latent heat due to water vapor condensation, and sensible heat of the liquid film cooling. Colburn, Hougen, and Drew considered only the sensible cooling and the latent heat of the water vapor condensation and neglected the liquid film sensible cooling. Ackerman considered the sensible

condensate cooling by applying a correction factor in the flue gas heat transfer coefficient. The Colburn and Drew equation with Ackerman correction factor for the surface element dA is given in equation (1):

$$\left[h_{fg} \times \varepsilon \times \left(T_{fg} - T_i\right) + N_t \times \lambda\right] \times dA = \left[U_o \times \left(T_i - T_{cw}\right) \ \right] \times dA \tag{1}$$

In the above equation, on the left, the first term refers to the sensible heat transfer from the flue gas to the heat exchanger tube, and the second term is water vapor latent heat transfer. h_{fg} represents the convective heat transfer coefficient on the flue gas side, ε is the Ackerman correction factor for heat transfer in the presence of mass transfer, and T_{fg} and T_i are the bulk temperature of flue gas and interface temperature, respectively. N_t is the water vapor condensate rate, and λ is the latent heat of water vapor evaporation. T_{cw} is the cooling water temperature, and U_o is the overall heat transfer coefficient.

The water vapor condensate rate N_t can be calculated from equation (2).

$$N_t = F * Ln\left[\frac{1 - Y_I}{1 - Y_G}\right] \tag{2}$$

Where Y_I and Y_G are the mole fraction of water vapor (as condensing gas) at the interface and gas bulk, respectively. F is the mass transfer coefficient and can be estimated using the heat and mass transfer analogy:

$$F = \frac{h_{fg}}{c_{p-fg} \times Le^{2/3}} \tag{3}$$

In the above equation, Le is the Lewis number of the water vapor in the flue gas and is calculated using equation (4).

$$Le = \frac{Sc}{Pr} = \frac{\alpha_{fg}}{D_{H_2o-gas}} \tag{4}$$

Where, Sc is Schmidt number, Pr is Prandtl number, α_{fg} is thermal diffusivity of flue gas, and D_{H_2o-gas} is diffusion coefficient of the water vapor into the flue gas.

Antoine's equation can be used to calculate Y_I at the interface. This equation gives the relationship between temperature and saturated pressure of vapor at the water vapor interface (Jeong, Kessen, Bilirgen & Levy, 2010):

$$Y_I = \frac{\exp\left(a - \frac{b}{T_i + c}\right)}{P_{tot}} \qquad \mathrm{a} = 16.262, \mathrm{b} = 3799.89 \text{ and } \mathrm{c} = 226.35 \tag{5}$$

And P_{tot} is the total pressure of the flue gas.

Ackerman's correction factor is calculated using equation (6).

$$\varepsilon = \frac{\frac{N_t \times c_{p-v}}{h_{fg}}}{1 - \exp\left(\frac{-N_t \times c_{p-v}}{h_{fg}}\right)} \tag{6}$$

According to the above equation, when there is no condensation ($N_t = 0$), the Ackerman correction factor equals 1. Thus, the heat transfer coefficient of flue gas in equation (1) does not change.

Thermal resistances in heat transfer are illustrated in figure (1). The overall heat transfer coefficient is found using equation (7) (Kakac & Liu, 1998), when the condensation film resistance is ignored.

$$U_o = \frac{1}{\frac{r_o}{r_i} \times \frac{1}{h_{cw}} + \frac{r_o}{k} \times ln\left(\frac{r_o}{r_i}\right) + \frac{1}{h_{fg}}} \tag{7}$$

Where k, r_o, r_i are thermal conductivity, outer radius, and inner radius of heat exchanger pipe, respectively. The flue gas heat transfer coefficient for in-line tube bundles can be found using equation (8) (Cengel, 2006).

$$h_{fg} = \frac{Nu_D \times k_{fg}}{d_o} \tag{8}$$

$$\mathrm{Nu_D} = 0.27 \times Re_{max}^{0.63} \times Pr^{0.36} \times (\mathrm{Pr/Pr_s})^{0.25} \qquad 1000 < \mathrm{Re_{max}} < 2 \times 10^5 \tag{9}$$

The flue gas Reynolds number can be found using following equation (Cortina, 2006).

$$\mathrm{Re_{max}} = \frac{\rho_{fg} \times d_o \times V_{fg-max}}{\mu_{fg}} \tag{10}$$

The cooling water heat transfer coefficient (h_{cw}) can be found using the following equations:

$$h_{cw} = \frac{Nu_{cw} \times k_{cw}}{d_i} \tag{11}$$

For water turbulent flow inside a smooth pipe, the Nusselt number is calculated using equation (12) (Cortina, 2006).

$$Nu_{cw} = 0.023 \times Re^{0.8} \times Pr^{0.4} \qquad Re > 10000 \tag{12}$$

$$Re = \frac{\rho_{cw} \times d_i \times V_{cw}}{\mu_{cw}} \tag{13}$$

$$V_{cw} = \frac{4 \times \dot{m}_{cw}}{\rho_{cw} \times \pi * {d_i}^2} \tag{14}$$

In order to model the heat and mass transfer from the flue gas in the CHE, the pipes of the CHE are divided into several cells with the length of dL. The cooling water and the flue gas are counter cross-flow in each cell and separated with the pipe wall. The heat and mass are transferred from the gas bulk to the gas-liquid interface and then are transferred to the cooling water. The output data of each cell is the input data for the next cell, and all needed variables in the referred equations are calculated for each cell separately.

The theoretical analysis was developed based on the following assumptions:

- CHE with counter cross flow
- One-dimensional, steady-state flow
- Vapor and non-condensable gases in the flue gas are well mixed and are at thermodynamic equilibrium.
- Condensing film thickness assumed as zero
- Film condensation in the CHE
- No heat loss from the CHE to the surroundings
- No fog formation in the gas phase

2.2 ORC Cycle

As shown in figure 2, the cooling water passing through the CHE is heated up by the flue gas stream and sent to the ORC cycle evaporator as an energy input source for electricity generation. As shown in figure 2, the heated water enters the ORC cycle (point i) evaporator from the CHE and vaporizes the cycle's working fluid (point 3). The superheated vapor is sent to the turbine, which is coupled to a power-producing generator. Working fluid leaves the turbine as a low-pressure vapor (point 4) and is condensed in the ORC cycle (point 1) condenser, and then the working fluid is pumped back to the evaporator. Figure 2 also shows the T-S diagram of the studied ORC cycle.

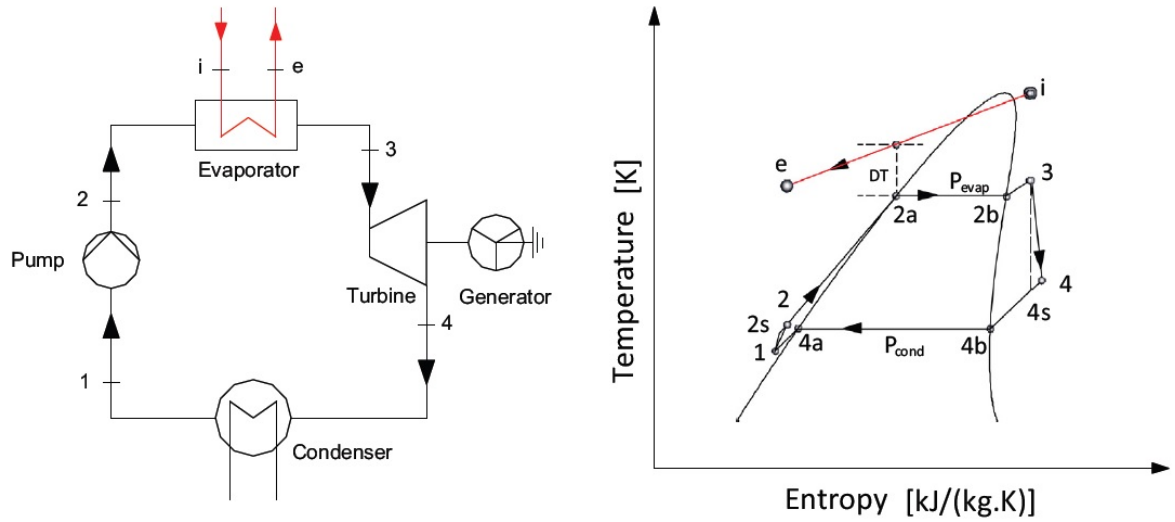

Figure 2. ORC cycle

The thermodynamic equations of the ORC cycle are written as below:

1. Evaporator:

$$\dot{Q}_{eva} = \dot{m}_r \times (h_3 - h_2) \tag{15}$$

2. Turbine:

$$\dot{W}_t = \dot{m}_r \times (h_3 - h_4) \tag{16}$$

3. Condenser:

$$\dot{Q}_{cond} = \dot{m}_r \times (h_4 - h_1) \tag{17}$$

4. Pump:

$$\dot{W}_p = \dot{m}_r \times (h_2 - h_1) \tag{18}$$

In the above equations, $\dot{Q}_{eva}$ and $\dot{Q}_{cond}$ are heat transfer rate in evaporator and condenser, respectively. $\dot{W}_t$ is the generated power by the turbine, and $\dot{W}_p$ is the consumed power by the pump. $\dot{m}_r$ is the mass flow rate of the working fluid, and h is the enthalpy.

The evaporator superheating can be determined using equation (19).

$$SH_{eva} = T_3 - T_{2b} \tag{19}$$

The net generated power by a turbine is calculated using equation (20).

$$\dot{W}_{net,t} = \dot{W}_t - \dot{W}_p \tag{20}$$

The recovered heat from the flue gas ($\dot{Q}_{recovered}$) or the transferred heat from CHE cooling water is calculated using equation (21).

$$\dot{Q}_{recovered} = \dot{m}_{cw} \times c_{p-cw} \times (T_i - T_e) \tag{21}$$

In the above equation, $\dot{m}_{cw}$ is the mass flow rate of the condensation in heat exchanger cooling water. T_i and T_e are the enter and exit temperature of cooling water to the ORC evaporator, respectively.

The turbine and pump isentropic efficiency is expressed using equation (22) and equation (23).

$$\eta_{is,t} = \frac{(h_3 - h_4)}{(h_3 - h_{4s})} \tag{22}$$

$$\eta_{is,p} = \frac{(h_{2s} - h_1)}{(h_2 - h_1)} \tag{23}$$

According to the thermodynamics first law, the ORC cycle thermal efficiency can be found using Eq. (24):

$$\eta_{cycle} = \frac{\dot{W}_{net,t}}{\dot{Q}_{recovered}} \tag{24}$$

3. System Description

In this study, a heat and water recovery unit for the flue gas of a thermal power plant boiler is designed. The main purpose of this study is to recover heat and water and use them in the process or elsewhere, namely recovered water for cooling tower makeup water and recovered heat for power generation through an ORC cycle. The exact data of the Bandar Abbas power plant are used in the theoretical analysis. Bandar Abbas power plant has four units with an equal capacity of 320 MWs. The recovery setup is designed for one unit. The boiler data of the studied unit is presented in Table (1).

Table 1. Bandar Abbas boiler data

Fuel	Fuel flow rate	Flue gas outlet temperature	Flue gas flow rate	Water vapor Volume concentration	Excess air
Natural gas	27000 m^3/hr	160 ℃	1190 ton/hr	13-17%	12%

Figure 3 shows the diagram of the thermal power plant and the heat and water recovery unit. The boiler exit flue gas is passed through a CHE. In this heat exchanger, the flue gas is cooled to a temperature lower than the dew point temperature of its water vapor.

The cooling water circulating in the CHE is heated by the transferred heat from the flue gas. Then, the heated cooling water is sent to the ORC cycle to evaporate and superheat the organic fluid of the ORC cycle. Then, the superheated fluid is expanded in the turbine of the cycle and leads to power generation. The condensed water in the CHE is collected and sent to the treatment unit and then is used as the cooling tower makeup water.

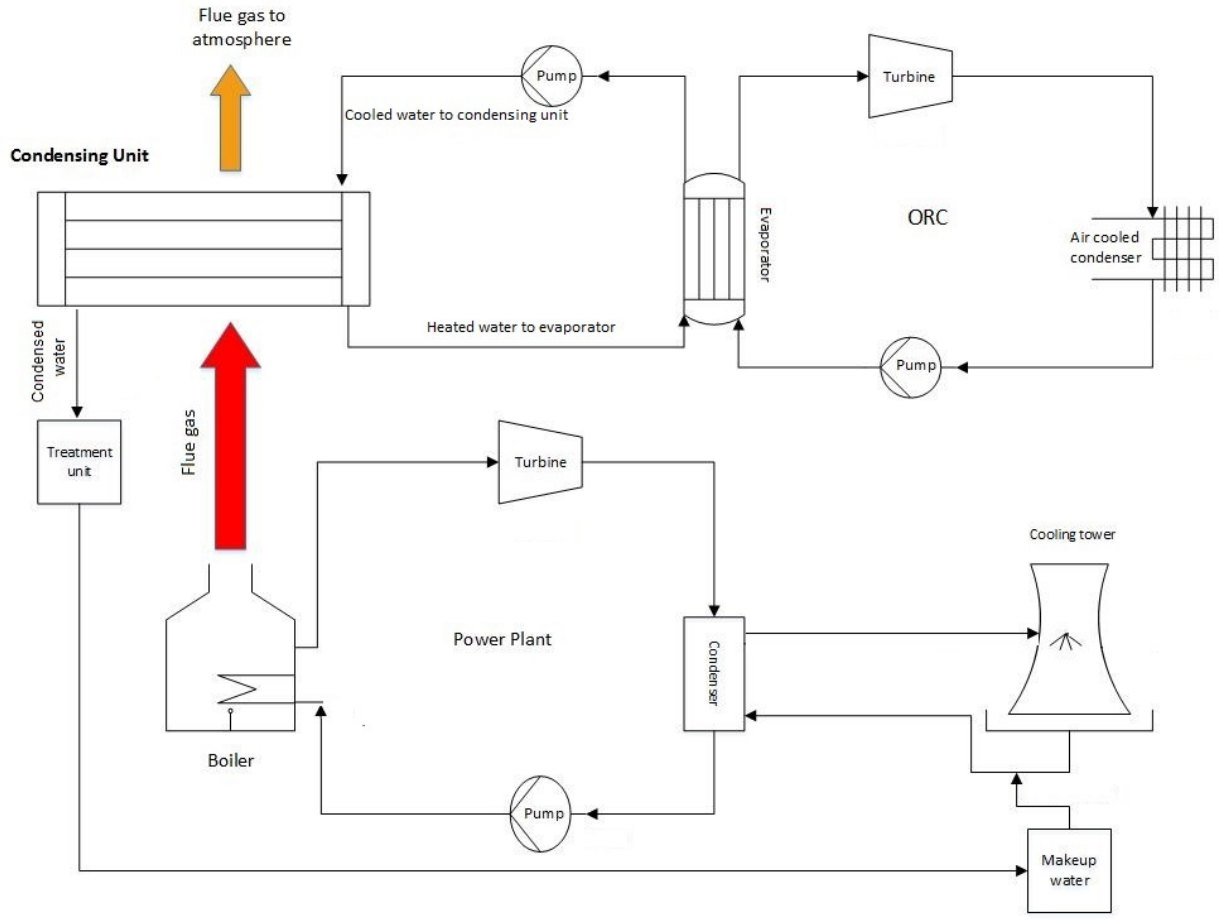

Figure 3. Diagram of power plant and heat-water recovery unit

4. Results

4.1 Condensing Heat Exchanger

A MATLAB code is developed to simulate the combined heat and mass transfer process in the condenser. The stream properties are calculated using REFPROP 9. The generated data by the code are verified using the data presented by Terhan and Comakli (2016), who designed a CHE for cooling and condensation process of the exhaust flue gas of a 60 MW boiler. Figure 4 compares our developed code and the one presented by Terhan and Comakli (2016). The flue gas is cooled from 158 ℃ to 40 ℃ , and the cooling water is heated from 10 ℃ to 60 ℃ in a counter-current manner. As shown in figure 4, the generated results of the code well align with those of Terhan and Comakli (2016).

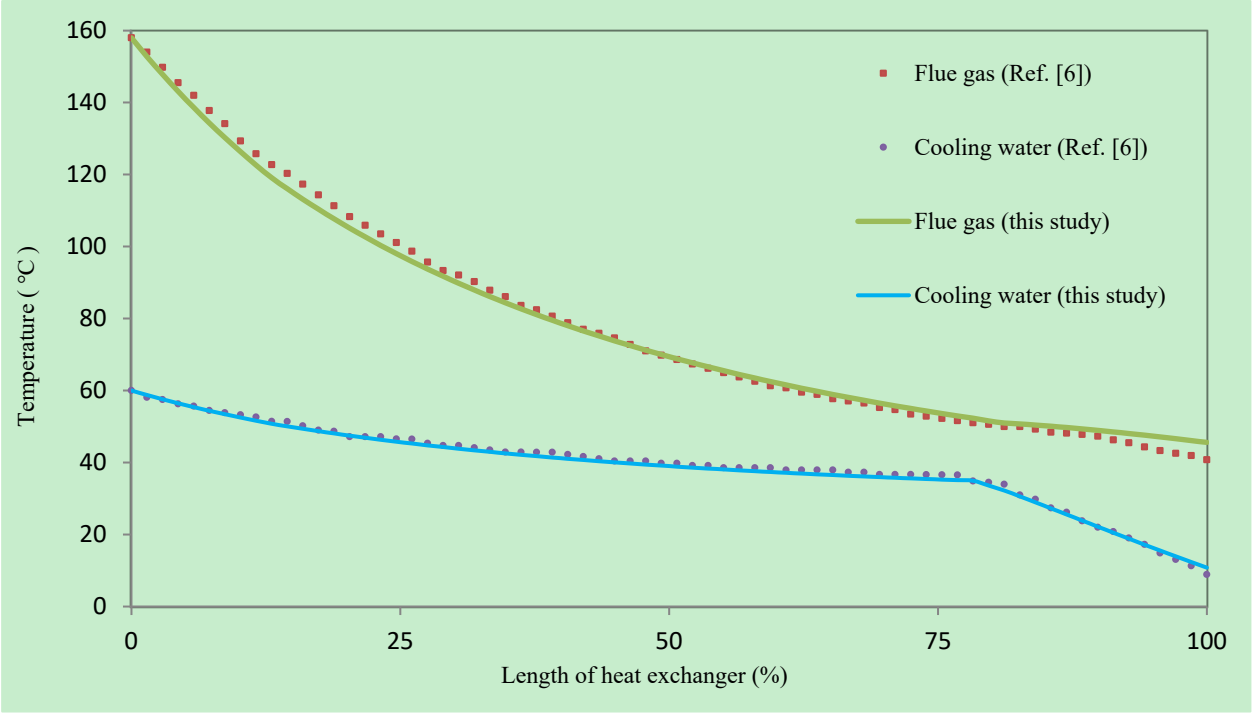

Figure 4. Comparison of the calculated temperature of flue gas and cooling water with results from Ref. [6]

Figure 5 shows the geometry of the designed counter-cross U-shaped CHE. The condensing unit includes 4 units with equal capacities. The design parameters of each condensing heat exchanger are listed in table 2.

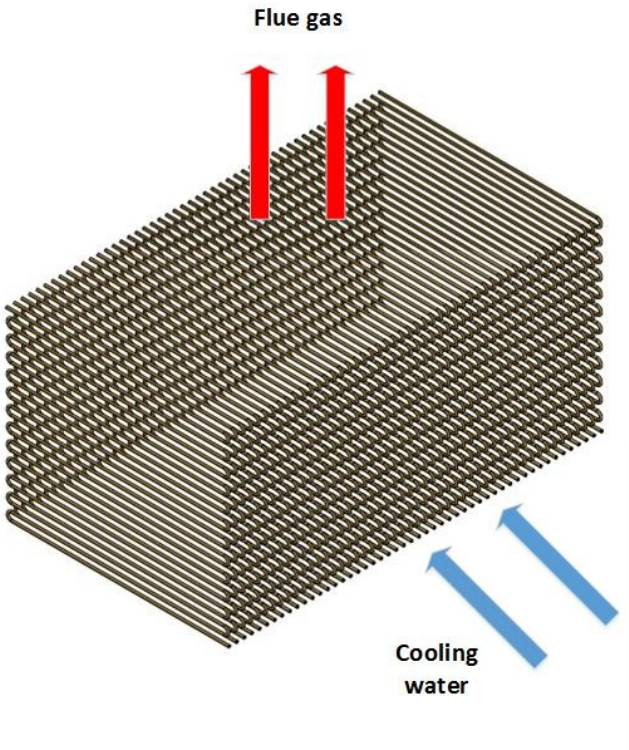

Figure 5. The geometry of a CHE

Table 2. Desinged CHE parameters

Parameter	Value
Flue gas mass flow rate	82.64 kg/s
Cooling water mass flow rate	82.64 kg/s
Pipe outer diameter	55.57 mm
Pipe inner diameter	50.80 mm
Number of tube bundles	60
Height of each pipe	6 m

The temperature change of the flue gas and the cooling water, along the length of the counter current CHE for 15% water vapor volume concentration, are shown in figure 6. As observed in the figure, the gas temperature reduces from 160 ℃ to 53.4 ℃, and the cooling water temperature increases from 27.15 ℃ to 80 ℃. The condensation occurs at 72.9% of the CHE length, and heat transfer rate increases by releasing the latent heat of the water vapor.

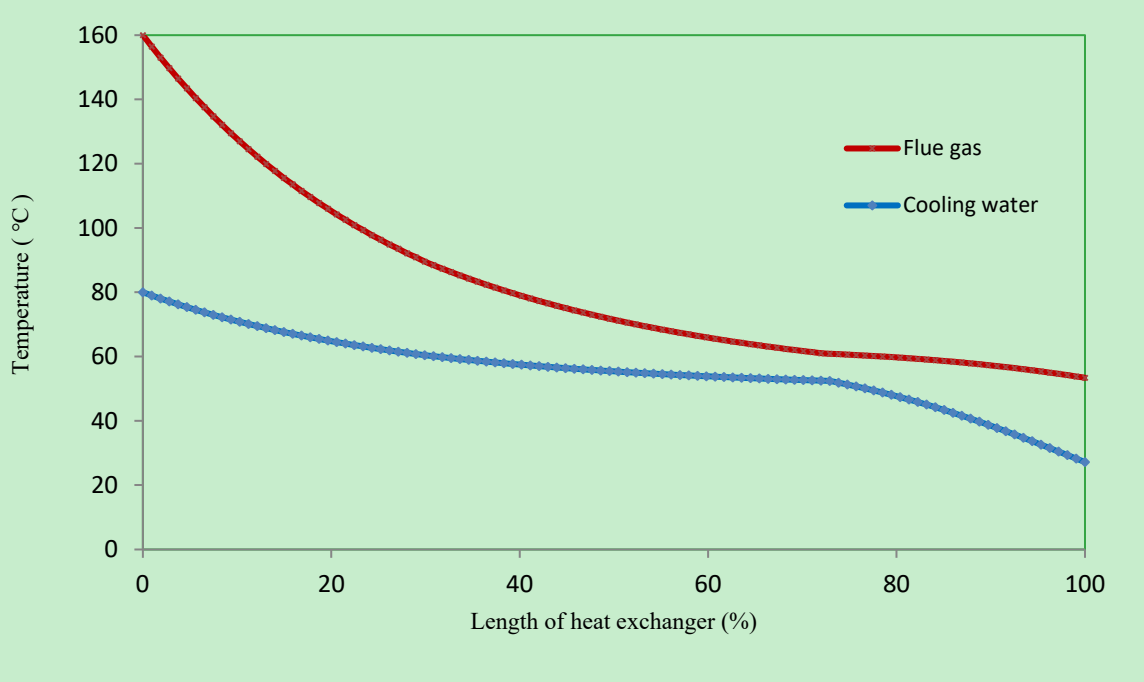

Figure 6. Flue gas and cooling water temperature change along the length of CHE

As shown in figure 3, the rejected heat from the CHE cooling water is used as the heat source for the ORC cycle. It is assumed that the cooling water inlet and outlet temperature in the CHE are 27.15 ℃ and 80 ℃, respectively. Table 3 lists The calculated temperature of the flue gas and the cooling water for different water vapor concentrations in the counter-cross condensing heat exchanger. As the amount of water vapor in the flue gas increases, condensation begins earlier at a higher temperature and increases latent heat transfer and a decrease in heat exchanger area requirement. The calculated area of designed heat exchangers for different water vapor concentrations is shown in figure 7.

Table 3. The calculated temperature in the heat exchanger

Water vapor volume concentration	None-condensing zone				Condensing zone			
	Inlet		Outlet		Inlet		Outlet	
	T_{fg}	$T_{c.w}$	T_{fg}	$T_{c.w}$	T_{fg}	$T_{c.w}$	T_{fg}	$T_{c.w}$
13 %	160	52.19	58	80	58	27.15	49.7	52.19
15 %	160	52.4	60.88	80	60.88	27.15	53.4	52.4
17 %	160	52.68	63.41	80	63.41	27.15	56.58	52.68

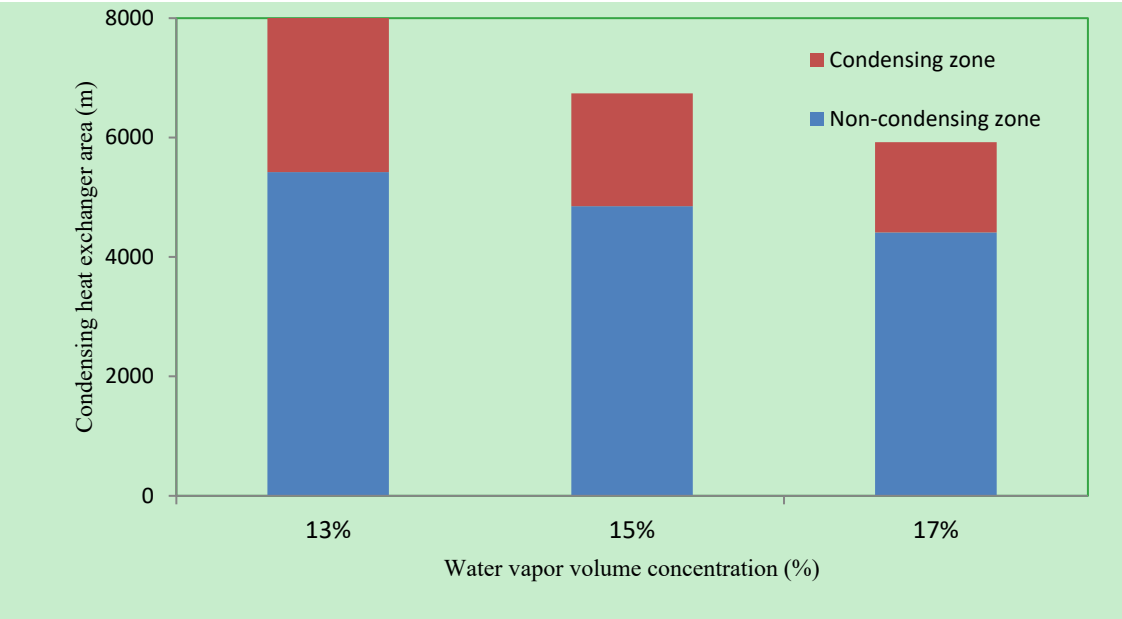

Figure 7. Area of designed condensing heat exchanger

Due to condensation, the mass transfer from the exhausted flue gases to the interface occurs, and thus the water vapor mole fraction decreases in the gas bulk. As a result, the non-condensable gases mole fraction increases. Along the CHE length, non-condensable gasses accumulate at the interface, and then the water vapor mole fraction decreases. figure 8 shows the mole fraction change of water vapor and non-condensable gases and the CHE for 15 % water vapor concentration.

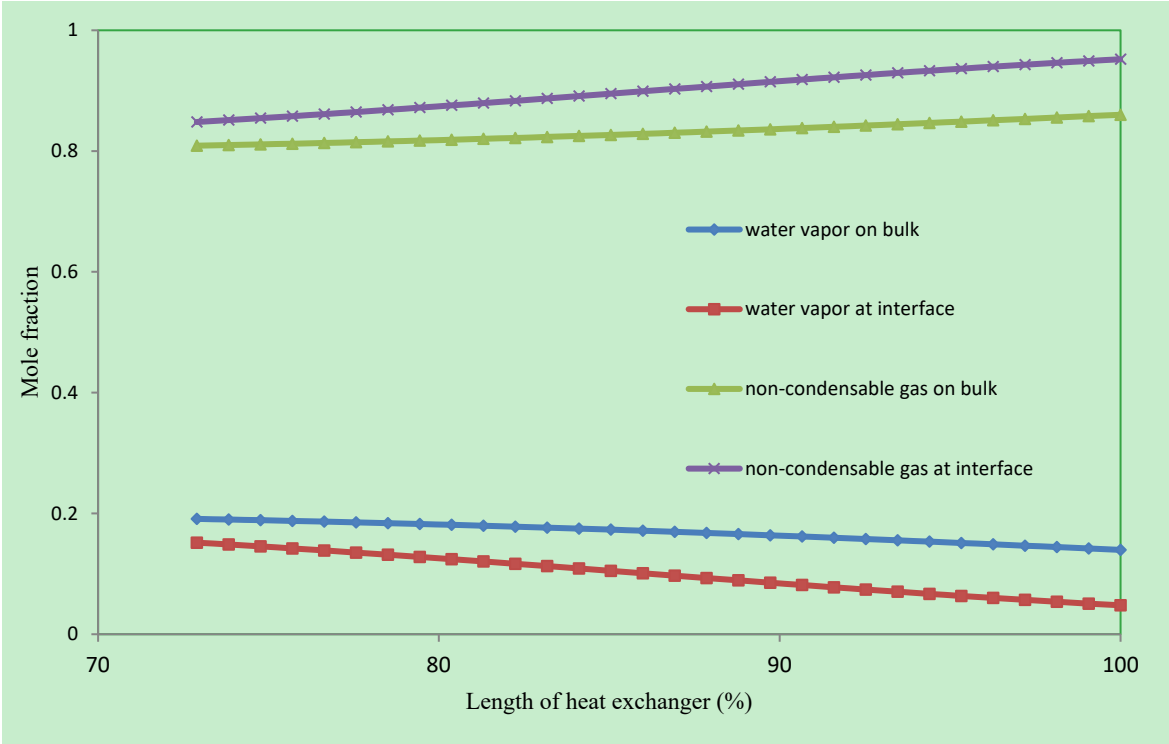

Figure 8. Change of mole fractions along the length of CHE

Figure 9 shows the amount of cumulative recovered heat in the condensing unit (including 4 condensing heat exchangers). Before condensation begins, the heat transfer rate decreases due to the decrease in temperature difference between the hot and cold streams. However, the heat recovery rate increases with the start of

condensation and latent heat transfer of the water vapor. As shown in Figure 9, for lower water vapor concentrations in the flue gas, a larger CHE length is exposed to the condensation and increases the condensing zone area. Due to corrosion problems in the condensing zones, higher price materials are used in manufacturing the tube bundles. Thus, with an increase in condensing zone area, the manufacturing cost will increase.

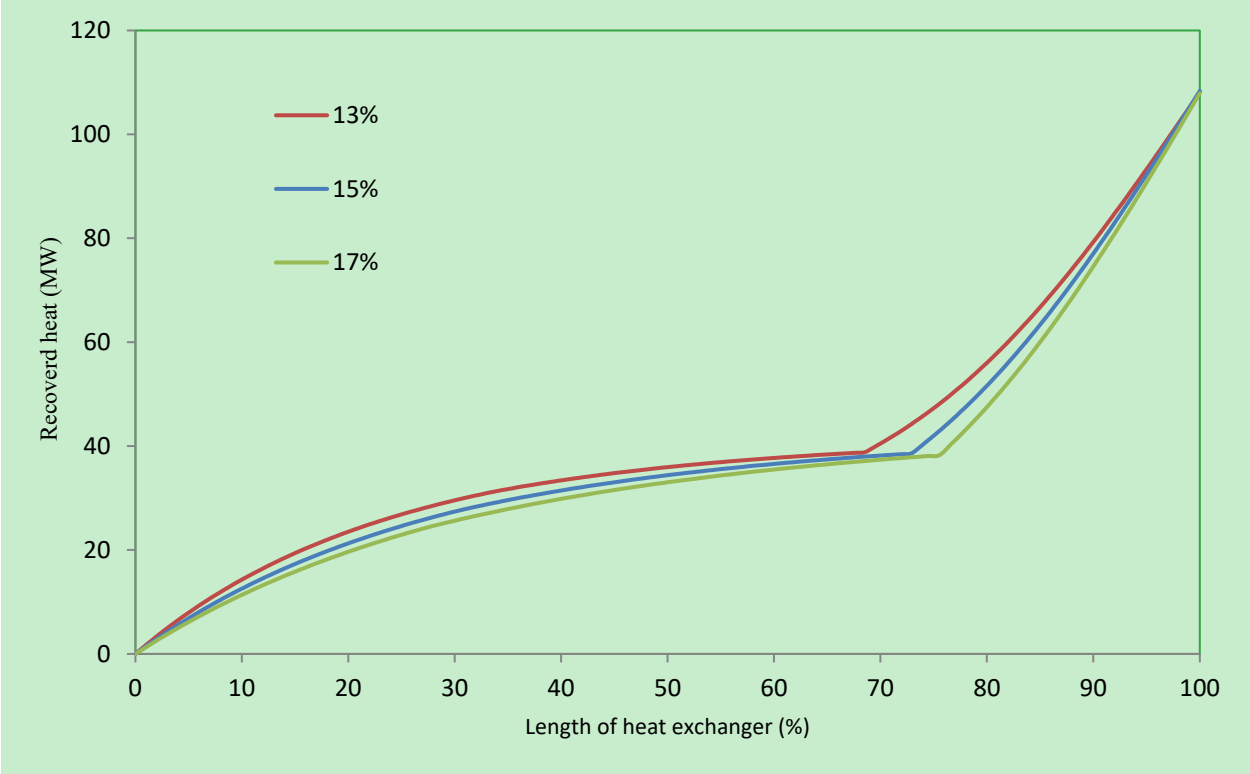

Figure 9. Cumulative recovered heat along the condensing unit

Figure 10 shows the mass flow rate of the condensed water along the CHE length. As shown in Figure 10, approaching the end of the heat exchanger reveals increases in the cumulative mass flow rate of the condensed water. In addition, the temperature of flue gas and also its water vapor content decreases towards the end of the condensing zone. Meantime, the flue gas faces cooling water with lower temperature (at the inlet) towards the exit point. Although the cumulative condensation increases along the condenser, the condensation decreases toward the end of the condenser due to the reduction of water vapor content. This, in turn, causes an increase in the concentration of non-condensable gases at the interface of the liquid film and the gas bulk.

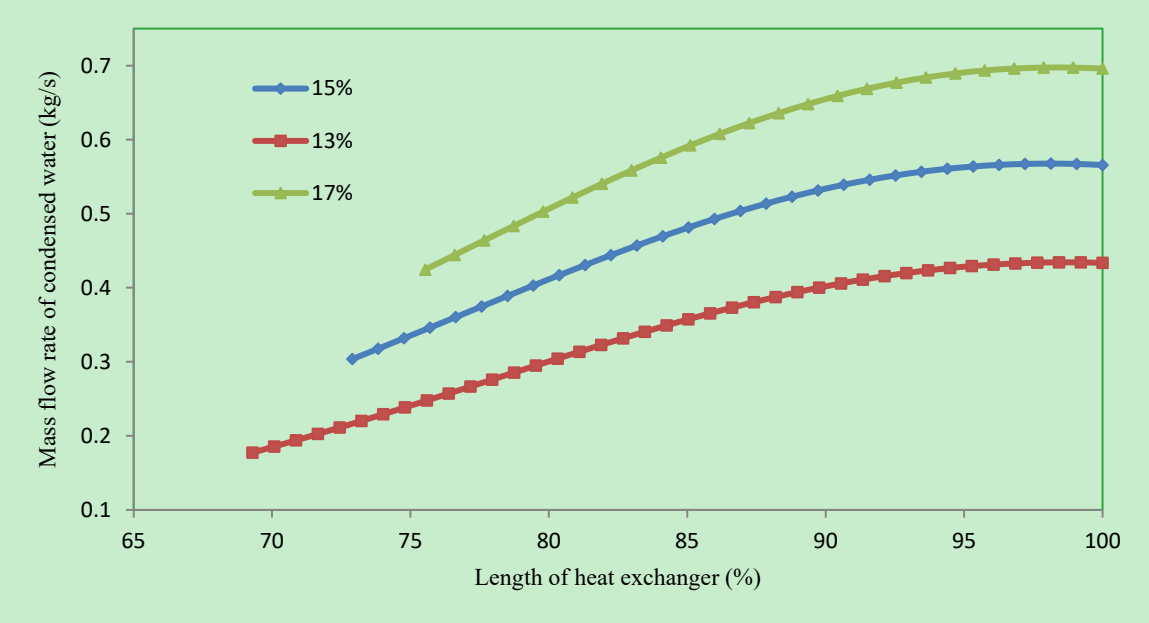

Figure 10. Mass flow rate of condensed water along the CHE

Table 4 presents the amount of water that could be recovered from a 320 MW natural gas-fired power plant based on different water vapor concentrations. In a 320 MW power plant, the water evaporation rate in the cooling tower is 107.5 kg/s. According to Table 4, almost 14% of the cooling tower makeup water could be saved using the condensing unit.

Table 4. Recovered water mass flow rate in the condensing unit

Water vapor concentration (%)	13	15	17
Recovered water (kg/s)	13.98	14.39	14.67

4.2 ORC cycle

The ORC cycle operating conditions are given in Table 5. It is essential to consider the pintch point between the ORC cycle working fluid and the hot water from condensing heat exchanger for maximum heat recovery from the hot stream. The pintch point is a key factor for the ORC cycle performance and should be as low as possible to increase the cycle efficiency. However, this will increase the evaporator heat transfer area and capital cost. The calculations in this study were made for pintch point of 3-k at the evaporator.

The RC318 is chosen as the working fluid due to its good performance in low-temperature heat sources and low environmental damage. The heated water temperature originating from the condensed heat exchanger to the evaporator is 80 ℃ for all calculations. The following calculations are based on varying evaporation temperatures as a key parameter for ORC cycle efficiency.

Table 5. ORC cycle input data

Parameter	Value
Condensing temperature	25 ℃
Condenser sub-cooling	3 ℃
Evaporator superheating temperature	5 ℃
Evaporator pinch temperature	3 ℃
Turbine and pump isentropic efficiency	85 %
Inlet heated water temperature to evaporator	80 ℃
Heated water mass flow rate	330.5 kg/s

Figure11 shows the evaluation of the ORC net generated power as a function of evaporation temperature. It should be noted that the net generated power is maintained by the turbine if the pump power consumption is considered almost negligible. As shown in figure11, the net power first increases and then decreases by increasing the evaporation temperature. This can be explained by referring to equation (16). The power produced by the turbine depends on two terms that change differently with the evaporation temperature. The cycle working fluid mass flow rate decreases when evaporation temperature decreases, and the enthalpy difference term " h3 – h4" increases when the evaporation temperature increases. The optimum net-generated power can be achieved in an evaporation temperature of 50 ℃.

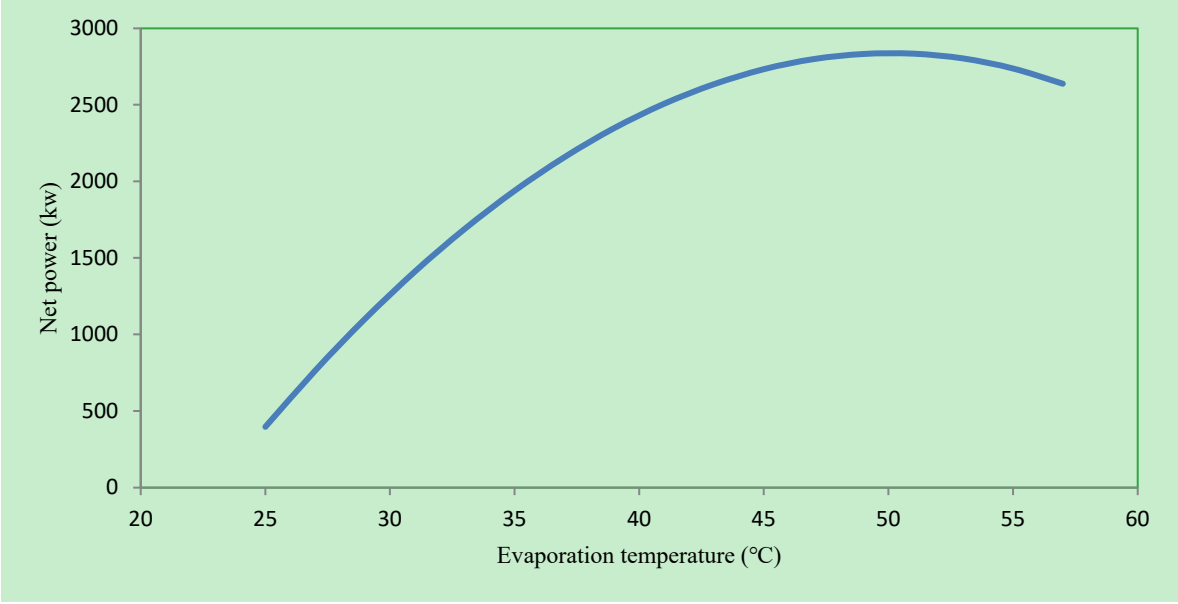

Figure 11. ORC generated power change by increasing evaporator temperature

As figure 12 illustrates, the rise in the evaporator operating temperature would increase the circulating water temperature (cooling water circulating the condensing heat exchanger as a cooler and the evaporator as a heater). By raising the temperature of this circulating water at the evaporator inlet to maintain better performance, the temperature of the water leaving the evaporator increases as the energy source for the ORC cycle. Accordingly, due to the constant temperature of the flue gas, the heat amount (and heat due to the recovered mass) in the CHE decreases.

This finding is also noted by referring to figure 6 The flue gas temperature leaving the CHE decreases as a result of the increase in inlet cooling water temperature. Thus, less water vapor could be condensed in the CHE. Fig.13 shows the decrease in water vapor recovery efficiency due to increasing the evaporation temperature. The

maximum water recovery efficiency occurs at an evaporation temperature of 25 ℃ . Water vapor's maximum recovery efficiency is 38% for 13% water vapor volume in the flue gas.

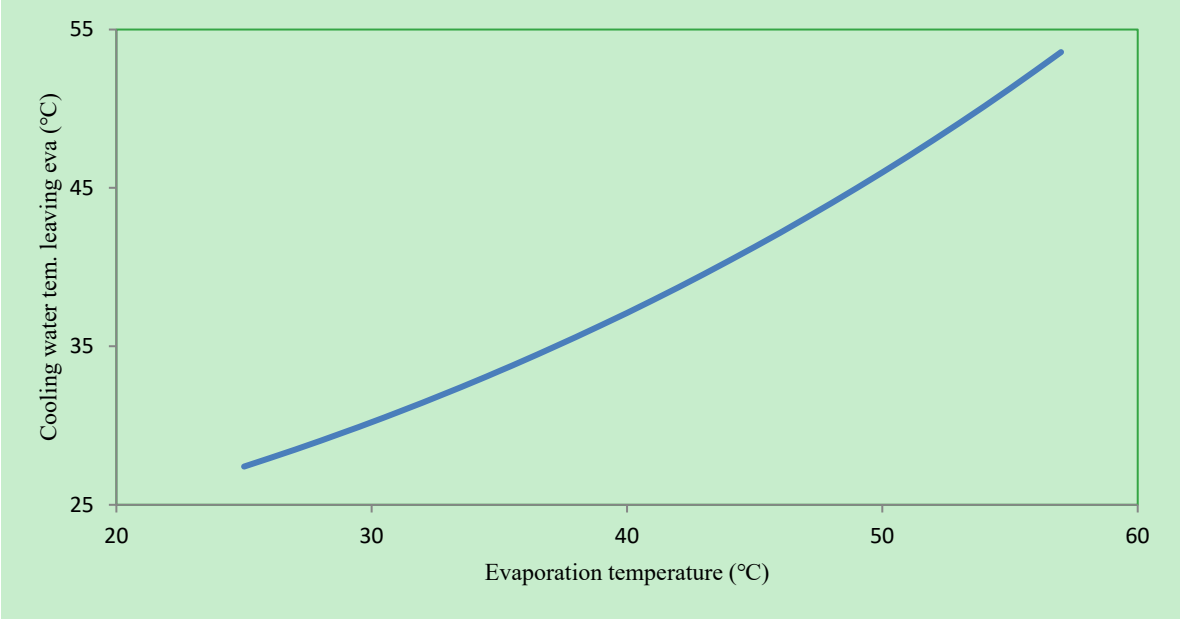

Figure 12. Evaluation of cooling water temperature leaving evaporator by increasing the evaporation temperature

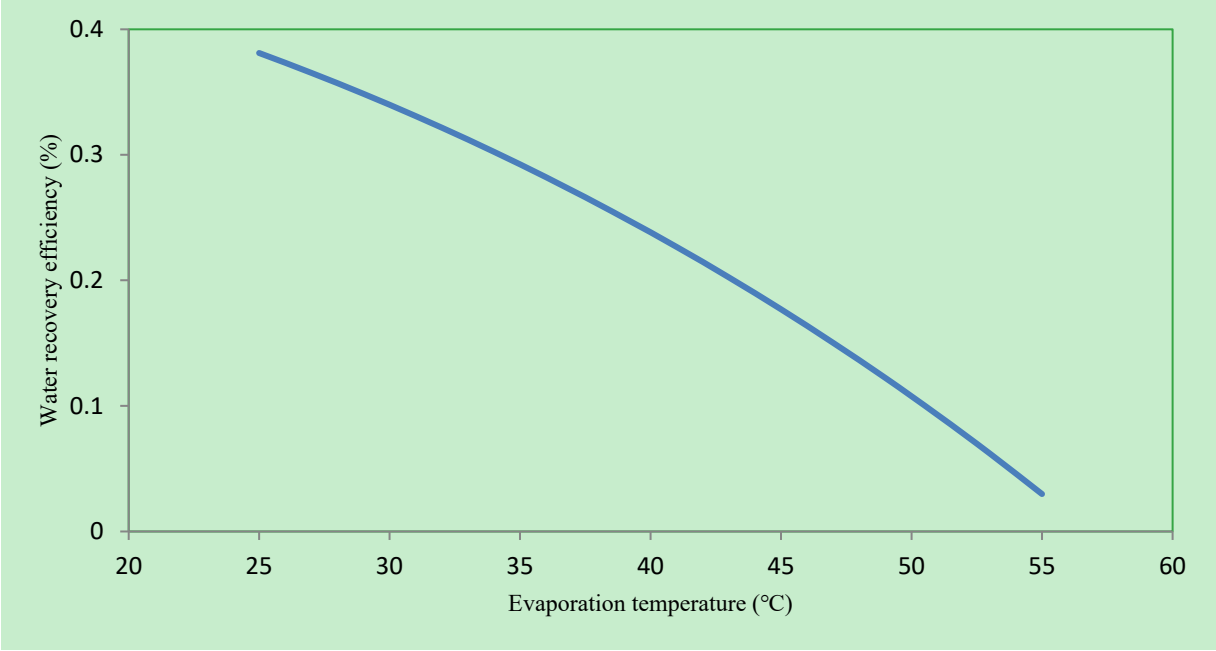

Figure 13. Water vapor recovery efficiency by increasing evaporation temperature

Figure14 shows the evaluation of ORC cycle efficiency by increasing the evaporation temperature. By increasing the evaporation temperature, the evaporator heat load decreases and leads to an increase in the ORC efficiency.

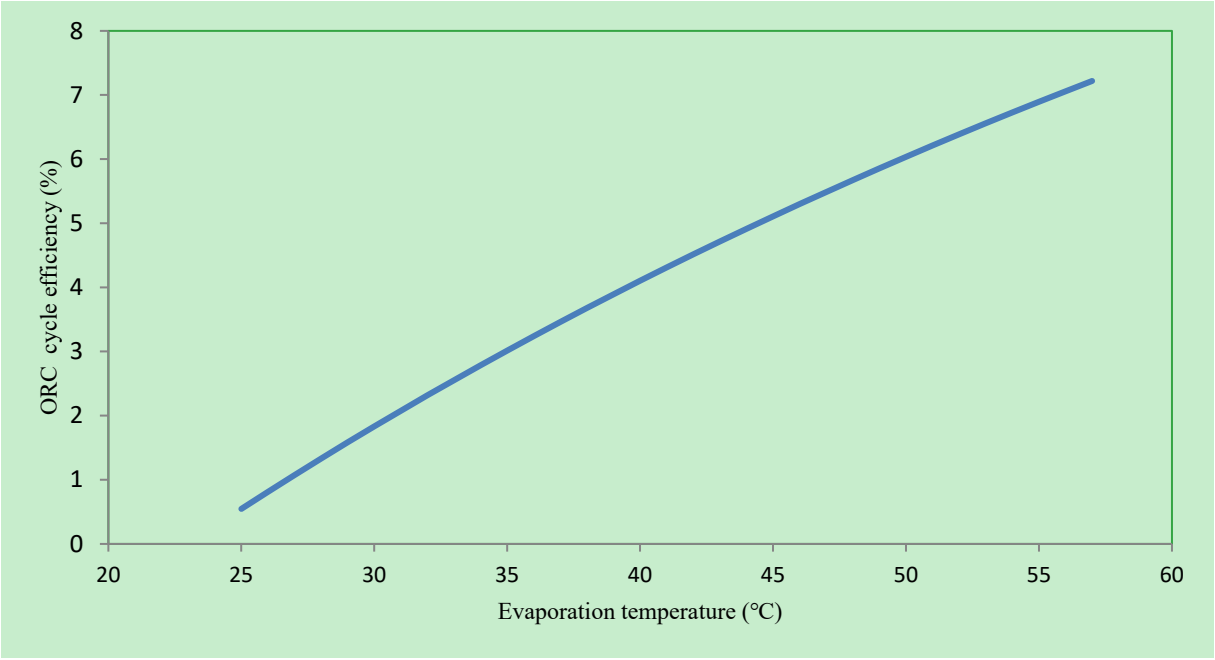

Figure 14. ORC cycle efficiency by increasing the evaporation temperature

5. Conclusion

In this study, water and heat recovery from the boiler's exhaust gases in the Bandar Abbas power plant was investigated. In the Bandar Abbas power plant, the boiler flue gases are discharged to the atmosphere at a temperature of 160 ℃ and 13-17 % flue gas volume of water vapor. Using film theory and a heat and mass transfer analogy, we designed a condensing heat exchanger to recover the flue gas's heat and water vapor content in the shell and applied cooling water as a coolant passing through the condenser tubes. In this process, the flue gas temperature is reduced to a level below its dew point. Accordingly, heat and mass are recovered from the flue gases.

A condensing unit consisting of 4 condensing heat exchangers was designed for a 320 MW unit of the power plant. The recovered heat by the cooling water was used as the heat source of the ORC cycle, and up to 2.8 MW power was produced depending on the evaporation temperature. After treatment, the recovered water was used as makeup water in the cooling tower of the power plant and saved almost14 % of water consumption.

Several studies were carried out based on the volume percentage of water vapor in the flue gases. Mostly, they found that with increasing water vapor, water recovery efficiency increases, and the size of both condensing and non-condensing zones decreases. Also, a parametric analysis was performed based on evaporation temperature changes from 25 ℃ to 57 ℃. It was found that with increasing the evaporation temperature, the power production of the ORC cycle first increases and then decreases. The water vapor recovery efficiency decreases in the condensing heat exchanger, and the ORC cycle efficiency increases. Therefore, in addition to thermodynamic and thermal analysis, optimization should be done based on the amount of water recovery and power production.

Nomenclature

A	Heat transfer area [m^2]
c_{p-cw}	Specific heat of cooling water [kJ/kg K]
c_{p-fg}	Specific heat of flue gas [kJ/kg K]
D_{H_2o-gas}	Mass diffusivity of water vapor in flue gas [m^2/s]
d_o	Outer diameter of tube [m]
F	Mass transfer coefficient
h	Enthalpy [kj/kg]
h_{cw}	Heat transfer coefficient of cooling water side [W/m^2 K]
h_{fg}	Heat transfer coefficient of flue gas [W/m2 K]

k	Thermal conductivity [W/m K]
Le	Lewis number
$\dot{m}_{cw}$	Mass flow rate of cooling water [kg/s]
$\dot{m}_r$	Mass flow rate of ORC [kg/s]
Nu	Nusselt number
N_t	Water vapor condensate rate [kg/s.m^2]
P	Pressure [Pa]
Pr	Prandtl number
$\dot{Q}$	Heat load [kW]
r_i	Inner radius [m]
r_o	Outer radius [m]
Re	Reynolds number
Sc	Schmidt number
T	Temperature [℃]
U_o	Overall heat transfer coefficient [W/m^2 K]
V	Velocity [m/s]
Y	Mole fraction
$\dot{W}$	Power [kW]

Greek symbols

α	Thermal diffusivity [m^2/s]
ε	Ackerman's correction factor
η	Efficiency
λ	Latent heat [kj/kg]
ρ	Density [kg/m^3]

Subscripts

cw	Cooling water
cond	Condenser
CHE	Condensing heat exchanger
CHP	Combined heat and power
eva	Evaporator
fg	Flue gas
i	Interface
is	Isentropic
ORC	Organic Rankine cycle
p	Pump
SH	Super heating
tot	Total
v	Vapor

Conflicts of interests

We declare NO affiliations with or involvement in any organization or entity with any financial (such as honoraria, educational grants, participation in speakers' bureaus, membership, employment, consultancies, stock ownership, or other equity interest, and expert testimony or patent-licensing arrangements), or non-financial interests (such as personal or professional relationships, affiliations, knowledge or beliefs) in the subject matter or materials discussed in this manuscript.

References

Cengel, Y.A. (2006). *Heat and Mass Transfer, third edition*. McGraw-Hill, New York, United States.

Chen, Q., Finney, K., Li, H., Zhang, X., Zhou, J., Sharifi, V., & Swithenbank, J. (2012). Condensing boiler applications in the process industry, *Applied Energy, 89*, 30-36. https://doi.org/10.1016/j.apenergy.2010.11.020

Cho, E., Lee, H., Kang, M., Jung, D., Lee, G., Lee, S., Kharangate, C.R., Ha, H., Huh, S. & Lee, H. (2022). A neural network model for free-falling condensation heat transfer in the presence of non-condensable gases. *International Journal of Thermal Sciences, 171*, 107202. https://doi.org/10.1016/j.ijthermalsci.2021.107202

Comakli, K. (2008). Economic and environmental comparison of natural gas fired conventional and condensing combi boilers. *Journal of Energy Institute, 81*,242–246. https://doi.org/10.1179/014426008X371031

Cortina, M. (2006). *Flue gas condenser for biomass boilers (MSc Thesis)*. Lulea University of Technology, Lulea, Sweden.

Goel, N. (2012). *Design and performance analyses of condensing heat exchangers for recovering water and waste heat from flue gas (MSc Thesis)*. University of Lehigh, Pennsylvania, United States.

Gundermann, M., Raab, F., Raab, D. & Botsch, T.W. (2021). Investigation of the heat transfer coefficient during the condensation of small quantities of water vapor from a mixture with a high proportion of non-condensable gas in a horizontal smooth tube. *International Journal of Heat and Mass Transfer, 170*, 121016. https://doi.org/10.1016/j.ijheatmasstransfer.2021.121016

Huang, F., Zheng, J., Baleynaud, J.M., & Lu, J. (2017). Heat recovery potentials and technologies in industrial zones. *Journal of Energy Institute, 90*, 951–961. https://doi.org/10.1016/j.joei.2016.07.012

Jeong, K., Kessen, M.J., Bilirgen, H., & Levy, E.K. (2010). Analytical modeling of water condensation in condensing heat exchanger. *International Journal of Heat and Mass Transfer, 53*, 2361-2368. https://doi.org/10.1016/j.ijheatmasstransfer.2010.02.004

Kakac, S., & Liu, H. (1998). *Heat Exchangers: Selection, Rating and Thermal Design*. CRC Press, New York, United States.

Kessen, M. J. (2012). *Optimal design of an air-cooled condenser for flue gas from a power plant (PhD Thesis)*. University of Lehigh, Pennsylvania, United States.

Levy, E., Bilirgen, H., Jeong, K., Kessen, M., Samuelson, C., & Whitcombe, C. (2008). *Recovery of water from boiler glue gas*. Final technical report , Energy Research Center, University of Lehigh, Pennsylvania, United States.

Levy, E., Bilirgen, H., Kessen, M., Hazell, D., & Carney, B. (2011). Heat exchangers for cooling boiler flue gas to temperatures below the water vapor dew point, Technical Presentation (POWER2011-55106) at ASME Power Conference. https://doi.org/10.1115/POWER2011-55106

Li, K., Wang, E., Li, D., Husnain, N., & Fareed, Sh. (2019). Numerical and experimental investigation on water vapor condensation in turbulent flue gas. *Applied Thermal Engineering, 160*, 114009. https://doi.org/10.1016/j.applthermaleng.2019.114009

Li, Y., Yan, M., Zhang , L., Chen, G., Cui, L., Song, Z., Chang, J., & Ma, C. (2016). Method of flash evaporation and condensation – heat pump for deep cooling of coal-fired power plant flue gas: Latent heat and water recovery, *Applied Energy, 172*, 17-117. http://dx.doi.org/10.1016/j.apenergy.2016.03.017

Maalouf, S., Ksayer, E. B. & Clodic, D. (2016). Investigation of direct contact condensation for wet flue-gas waste heat recovery using Organic Rankine Cycle. *Energy Conversion and Management, 107*, 96-102. https://doi.org/10.1016/j.enconman.2015.09.047

Mohammadaliha, N., Amini, M. & Bahrami, M. (2020). Thermal performance of heat and water recovery systems: Role of condensing heat exchanger material. *Cleaner Engineering and Technology, 1*, 100024. https://doi.org/10.1016/j.clet.2020.100024

Nabati, H. (2011). Investigation on numerical modeling of water vapor condensation from flue gas with high CO2 cotent. *Energy and Power Engineering, 3*, 181-189. https://doi.org/10.4236/epe.2011.32023

Terhan, M., & Comakli, K. (2016). Design and economic analysis of a flue gas condenser to recover latent heat from exhaust flue gas. *Applied Thermal Engineering, 100*, 1007-10015. https://doi.org/10.1016/j.applthermaleng.2015.12.122

Wang, C., He, B., Sun, S., Wu, Y., Yan, N., Yan, L., & Pei, X. (2012). Application of a low pressure economizer for waste heat recovery from the exhaust flue gas in a 600 MW power plant. *Energy, 48*, 196–202. https://doi.org/10.1016/j.energy.2012.01.045

Xiong, Y., Niu, Y., Tan, H., Liu, Y., & Wang, X. (2014). Experimental study of a zero water consumption wet FGD system. *Applied Thermal Engineering, 63*, 272–277. https://doi.org/10.1016/j.applthermaleng.2013.10.047

Zhao, S., Yan, S., Wang, D.K., Wei, Y., Qi, H., Wu, T., & Feron, P.H.M. (2017). Simultaneous heat and water recovery from flue gas by membrane condensation: Experimental investigation. *Applied Thermal Engineering, 113*, 843–850. https://doi.org/10.1016/j.applthermaleng.2016.11.101